Patterning Chronic Active Demyelination in Slowly Expanding/Evolving White Matter MS Lesions

C. Elliott, D.L. Arnold, H. Chen, C. Ke, L. Zhu, I. Chang, E. Cahir-McFarland, E. Fisher, B. Zhu, S. Gheuens, M. Scaramozza, V. Beynon, N. Franchimont, D.P. Bradley, and S. Belachew

ABSTRACT

BACKGROUND AND PURPOSE: Slowly expanding/evolving lesions measured by conventional T1-weighted/T2-weighted brain MR imaging may contribute to progressive disability accumulation in MS. We evaluated the longitudinal change in myelin and axonal tissue integrity in white matter slowly expanding/evolving lesions by means of the magnetization transfer ratio and DTI radial diffusivity.

MATERIALS AND METHODS: Slowly expanding/evolving lesions were detected within the Study to Assess the Efficacy, Safety, Tolerability, and Pharmacokinetics of BIIB033 in Participants With Relapsing Forms of Multiple Sclerosis When Used Concurrently With Avonex (SYNERGY) Phase 2 clinical trial dataset (NCT01864148), comprising patients with relapsing-remitting and secondary-progressive MS ($n = 299$) with T1-weighted/T2-weighted MR imaging at all trial time points (baseline to week 72).

RESULTS: Compared with non-slowly expanding/evolving lesions (areas not classified as slowly expanding/evolving lesion) of baseline nonenhancing T2 lesions, slowly expanding/evolving lesions had a lower normalized magnetization transfer ratio and greater DTI radial diffusivity, both in patients with relapsing-remitting MS ($n = 242$) and secondary-progressive MS ($n = 57$, $P < .001$ for all). Although the changes with time in both the normalized magnetization transfer ratio and DTI radial diffusivity between slowly expanding/evolving lesions and non-slowly expanding/evolving lesions were positively correlated ($P < .001$), a decrease in the normalized magnetization transfer ratio and a greater increase in DTI radial diffusivity were observed in slowly expanding/evolving lesions versus non-slowly expanding/evolving lesions from baseline to week 72 in relapsing-remitting MS and secondary-progressive MS ($P < .001$ for all).

CONCLUSIONS: Patterns of longitudinal change in the normalized magnetization transfer ratio and DTI radial diffusivity in slowly expanding/evolving lesions were consistent with progressive demyelination and tissue loss, as seen in smoldering white matter MS plaques.

ABBREVIATIONS: MT = magnetization transfer; MTR = magnetization transfer ratio; nMTR = normalized MTR; nT1 = normalized T1; RD = radial diffusivity; RRMS = relapsing-remitting multiple sclerosis; SEL = slowly expanding/evolving lesion; SPMS = secondary-progressive multiple sclerosis

Received February 26, 2020; accepted after revision May 31.

From NeuroRx Research (C.E., D.L.A.) Montreal, Quebec, Canada; Department of Neurology and Neurosurgery (D.L.A.), McGill University, Montreal, Quebec, Canada; and Biogen (H.C., C.K., L.Z., I.C., E.C.-M., E.F., B.Z., S.G., M.S., V.B., N.F., D.P.B., S.B.), Cambridge, Massachusetts.

This research was funded by Biogen, Cambridge, Massachusetts.

Please address correspondence to Colm Elliott, PhD, NeuroRx Research, Montreal, QC, Canada, 3575 Parc Ave, Suite 5322, Montreal, QC, H2X 3P9, Canada; e-mail: celliott@neurorx.com

http://dx.doi.org/10.3174/ajnr.A6742

Chronic active lesions, or smoldering plaques, are a neuropathologic hallmark of chronic inflammation in MS[1] and are not found in neuromyelitis optica spectrum disorders[2] or chronic cerebrovascular diseases.[3]

Pathologically, chronic active lesions are typified by a "rim" of activated microglia and/or macrophages that may contain iron; they have altered morphology, sparse T- and B-cells at the core, and a slow rate of ongoing demyelination and axonal loss.[1,4-7] Susceptibility-based MR imaging methods have identified a hypointense paramagnetic rim that may reflect activity associated with iron accumulation and other MS-related pathology in the periphery of those chronic active white matter MS lesions.[4,8-11]

A method for automatic detection of slowly expanding/evolving lesions (SELs) on conventional T1-weighted/T2-weighted brain MR imaging was recently developed as a potential readout

of smoldering or chronic active plaques.[12] SELs are defined as contiguous regions of pre-existing T2 lesions showing constant and concentric local expansion, as assessed by the Jacobian determinant of the nonlinear deformation between reference and follow-up scans.[12] Furthermore, T1-weighted intensity-based measures of chronic white matter lesion tissue damage in SELs predict clinical progression in primary-progressive MS and may qualify as longitudinal in vivo neuroimaging correlates of progressive MS pathology.[13]

Practical guidelines recommend either paramagnetic rim identification on high-resolution T2* and phase MR imaging (7T or even 3T) or longitudinal T1-weighted/T2-weighted SEL detection for in vivo assessment of chronic active or smoldering lesions.[11] Paramagnetic rim lesion identification is a promising pathologic biomarker of iron/zinc accumulation in chronic active lesions.[14,15] In clinical trials and routine clinical practice settings, SEL detection may be more suitable for delivering quantitative measures of overall and lesion-level longitudinal change in tissue integrity associated with smoldering lesion inflammation, enabling the assessment of chronic lesion activity in datasets for which high-resolution T2* MR imaging is not available.

The magnetization transfer ratio (MTR) has previously been shown to associate strongly with myelin content,[16–19] especially in the absence of acute inflammation and edema. DTI can provide information about the orientation, size, and geometry of tissue integrity in white and gray matter in the brain and spinal cord.[20] DTI radial diffusivity (DTI-RD) has been proposed as a potential marker of overall myelination and/or tissue integrity in MS lesions.[21]

In this study, we used MTR and DTI-RD to evaluate longitudinal in vivo demyelination to further inform the pathologic understanding of chronic tissue damage in SELs of patients with relapsing-remitting MS (RRMS) and secondary-progressive MS (SPMS).[12]

MATERIALS AND METHODS

Trial Design, Patients, and MR Imaging Procedures

SELs[12] and non-SELs were determined in chronic white matter lesions of the pooled population (placebo and treatment groups) of the Study to Assess the Efficacy, Safety, Tolerability, and Pharmacokinetics of BIIB033 in Participants With Relapsing Forms of Multiple Sclerosis When Used Concurrently With Avonex (SYNERGY) trial (NCT01864148), a multicenter, randomized, double-blind, placebo-controlled, dose-ranging, parallel-group, Phase 2 study. Patients were randomly allocated in a 1:2:2:2:2 ratio to 1 of 5 parallel treatment groups of opicinumab (3, 10, 30, or 100 mg/kg) or placebo, once every 4 weeks for 72 weeks. Opicinumab is a human monoclonal antibody against LINGO-1, an inhibitor of oligodendrocyte differentiation and axonal regeneration.[22] All patients self-administered intramuscular interferon β-1a as a background anti-inflammatory treatment once a week, and approximately half of the population had not previously received MS disease-modifying therapies.[22] SYNERGY study details have been reported previously.[22] Eligible patients (18–58 years of age) had an Expanded Disability Status Scale score of 2–6 and relapsing MS, including RRMS and SPMS with relapses. Evidence of clinical or neuroimaging disease activity was required within 12 months before enrollment.[22]

Axial T1-weighted (3D spoiled gradient-echo, TR = 28–30 ms, TE = 511 ms, flip angle = 27°–30°, resolution = 1 × 1 × 3 mm), axial T2-weighted (2D fast spin-echo, TR = 4500–6200 ms, TE = 66–91 ms, resolution = 1 × 1 × 3 mm), axial MTR (2 consecutive 3D spoiled gradient-echo, TR = 32–62 ms, TE = 5–11 ms, flip angle = 10°–15°, resolution = 1 × 1 × 3 mm, with and without magnetization transfer pulse), and axial DTI (2D spin-echo echo-planar imaging sequence with a diffusion gradient, TR = 9800–16,000 ms, TE = 90–132 ms, b-values = 0 and 1000, 25–32 diffusion directions, resolution = 2.5 × 2.5 × 2.5 mm) were acquired at baseline and weeks 4, 8, 12, 16, 20, 24, 48, and 72.[22] Complete methods for brain MR imaging acquisitions are described in the On-line Appendix. The SEL analysis population ($n = 299$) represents the subset of the intention-to-treat population ($n = 418$) that had available T1-weighted and T2-weighted MR images at all aforementioned time points from baseline to week 72.

Identification of SELs

As previously described, SELs are detected as areas of T2 lesions, pre-existing at baseline, that show constant and concentric local expansion.[12] Before SEL detection, T2 lesions were identified in baseline scans using a semiautomated method,[23] in which a fully automated segmentation was subsequently manually reviewed and corrected by trained MR imaging readers. Identification of SELs is a 2-stage process. First, SEL candidates are identified as contiguous areas of pre-existing, nonenhancing T2 lesions that are ≥10 voxels in size and show local expansion from baseline to week 72; a minimum local expansion of 4% per year is used as a cutoff for determining SEL candidate boundaries, as in previous SEL analyses.[12] Local expansion is determined from the Jacobian determinant of the nonlinear deformation between the baseline and week 72 scans. Computation of the Jacobian is based on the pipeline proposed by Nakamura et al,[24] in which nonlinear registration is performed using the symmetric image normalization method,[25] and both T1-weighted and T2-weighted images are used for registration. The second stage of SEL detection scores each SEL candidate in turn, on the basis of the concentricity and constancy of expansion across time. Considering local expansion at all intermediate scans (weeks 4, 8, 12, 16, 20, 24, and 48) allows the identification of SEL candidates undergoing constant and gradual expansion across time; measuring concentricity allows identification of SEL candidates exhibiting inside-out radial expansion. Results pertaining to SEL analyses are presented for high-confidence SELs (with a heuristic score of ≥0).[12] Non-SELs are defined as complement regions from pre-existing, baseline, nonenhancing T2 lesions devoid of any SEL detection (irrespective of the heuristic score). SEL identification and all T1-weighted measures related to SELs and non-SELs were performed by NeuroRx Research staff, who remained blinded to all study patient-level information.

Normalization of T1-Weighted and MTR Signal Intensity

Before measuring T1-intensity change across time, T1WIs were normalized in a 2-stage process: 1) Least-trimmed squares normalized all serial T1WIs of a given patient to the baseline T1-

Baseline demographics and brain MR imaging characteristics of the SYNERGY SEL analysis population

	SEL Analysis Population[a]			Intention-to-Treat Population		
	RRMS	SPMS	All	RRMS	SPMS	All
No.	242	57	299	330	88	418
Median age (yr)	37.5	48.0	39.0	38.0	48.0	39.5
Female (%)	68	54	65	68	60	66
Mean (SD) number of T1 gadolinium-enhancing lesions	1.8 (4.7)	1.2 (3.7)	1.7 (4.5)	2.0 (4.7)	1.2 (3.3)	1.8 (4.4)
Patients with ≥1 T1 gadolinium-enhancing lesion (%)	45	30	42	46	31	43
Median nonenhancing T1-hypointense lesion volume (mL)	1.09	3.26	1.41	1.22	4.13	1.50
Median T2-hyperintense lesion volume (mL)	4.86	9.46	5.24	5.19	13.05	6.02
Median normalized brain volume (mL)	1447.9	1378.1	1426.1	1438.6	1367.0	1419.9
Median cortical gray matter volume (mL)	551.9	509.53	540.8	544.0	502.6	534.6

[a] The SEL analysis population ($n = 299$) represents the subset of the SYNERGY intention-to-treat population that had available T1-weighted and T2-weighted brain MR imaging scans at all time points from baseline to Week 72 (baseline and Weeks 4, 8, 12, 16, 20, 24, 48, and 72). For some time points, MTR and/or DTI-RD may not be available.

weighted scan, and 2) T1WIs for a given subject were linearly normalized by mapping the median gray matter T1 intensity at baseline to a value of zero and mapping the median normal-appearing white matter intensity at baseline to 1. Least-trimmed squares performs linear regression between coregistered sequential scans using the 50% of voxels whose least-squares fit has the smallest sum of squared residuals.[26] This process normalizes intensities within a given subject on the basis of only the subset of voxels that remain relatively unchanged with time. The first stage of normalization minimizes acquisition-related intensity variation across time for a given subject, whereas the second stage provides comparable measures of T1 intensity change across different subjects.

MTR intensities were calibrated by determining the median MTR values for both gray and white matter in a healthy control subject specific to each scanner. For each new-subject scan acquired in the same scanner, the MTR value corresponding to the median healthy control gray matter was mapped to zero, while the MTR value corresponding to the median healthy control white matter was mapped to 1. In normalized MTR images, a value of zero can thus be interpreted as corresponding to healthy (ie, non-MS) gray matter, while a value of 1 can be interpreted as corresponding to healthy white matter. DTI-RD is expressed in units of 10^{-3} mm^2/s and does not require normalization across scans.

Lesion-Level Visualization of Longitudinal Tissue Damage within a SEL Example

To display an example of lesion-level longitudinal tissue damage within discrete SELs, we modeled smooth voxel-based (linear fit) representations of normalized T1 (nT1), normalized MTR (nMTR), and DTI-RD intensity change across time in a high-confidence SEL. Heat map synthetic representations were produced that may represent biologic change and/or displacement. Linear models interpolating intensity change with time were used.

Statistical Analysis

The statistical analysis of SEL data was exploratory and included all patients from SYNERGY with no missing or nonevaluable T1-weighted and T2-weighted scans at any time point (baseline to week 72; SEL analysis population). No imputation of missing data was performed.

Continuous variables measuring tissue integrity (eg, MTR and DTI change from baseline in nMTR and DTI-RD) were compared between SELs and non-SELs using a Wilcoxon signed rank test, accounting for within-subject correlation of each variable. Change from baseline comparisons for continuous variables between patients with RRMS and SPMS were based on rank regression adjusted for covariates including baseline value, age, sex, and the baseline T2 volume category based on tertiles. Comparisons of baseline continuous variables between patients with RRMS and SPMS were based on rank regression, with MS type and covariates including age, sex, and baseline T2 volume category based on tertiles.

The Spearman rank correlation analysis was used to evaluate the association between change with time in continuous variables within SELs and non-SELs. Two-sided statistical tests were conducted at the 5% significance level without adjustment for multiplicity.

RESULTS

Baseline Demographics and Brain MR Imaging Characteristics of the SYNERGY SEL-Analysis Population

The baseline demographics and brain MR imaging characteristics of the SEL-analysis population from the SYNERGY dataset of patients with RRMS and SPMS are presented in the Table. The population was similar to the SYNERGY intention-to-treat population. In the SEL analysis population, patients with SPMS ($n = 57$) were ~10 years older and had a lower level of acute lesions as measured by the presence of gadolinium-enhancing T1 lesions and a 2-fold greater volume of baseline total T2 hyperintense lesions compared with patients with RRMS ($n = 242$). In addition, the baseline normalized brain volume and cortical gray matter volume were numerically lower, and a more balanced sex ratio was observed in the SPMS subgroup compared with patients with RRMS.

SEL Prevalence in RRMS versus SPMS

The proportion of patients with ≥1 SEL detected from baseline to week 72 was similar in patients with SPMS (89%) and RRMS (83%); a numerically greater proportion of patients with SPMS had >10 SELs (Fig 1*A*). Patients with SPMS had an overall greater number of SELs compared with patients with RRMS (median, 7.0 versus 4.0; Fig 1*B*), and an approximately 2-fold greater T2 volume of SELs (median at baseline, 718.2 versus 311.9 mm^3; Fig 1*C*); however, when accounting for differences in age, sex, and baseline total T2 hyperintense lesion volume, the differences

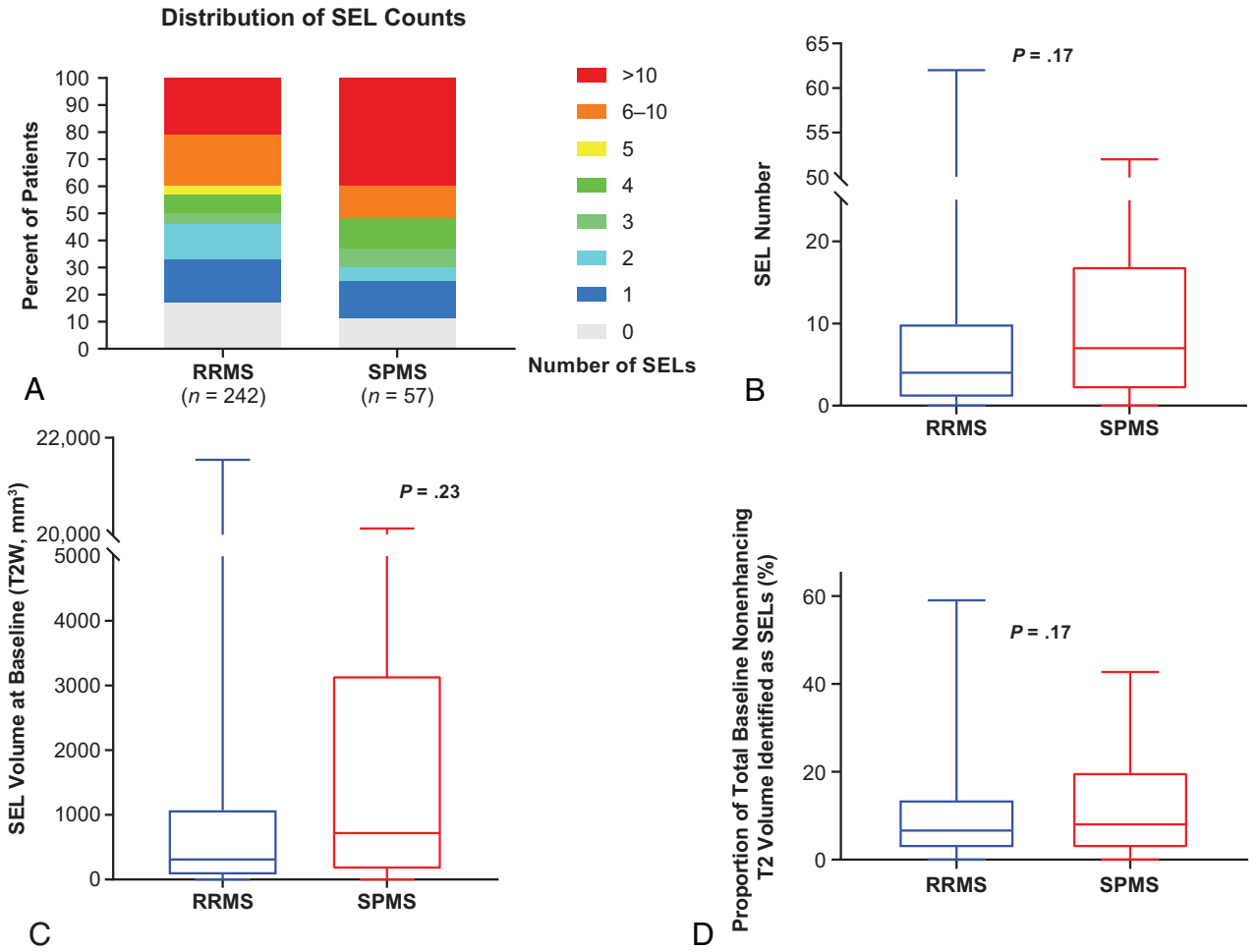

FIG 1. SEL prevalence in patients with RRMS and SPMS in SYNERGY. *A*, Frequency distribution (percentage) of patients with various levels of SEL counts. Boxplot representations of SEL number (*B*), SEL volume at baseline (*C*), and the proportion of total baseline nonenhancing T2 volume identified as SELs in SYNERGY in patients with RRMS ($n = 242$) and SPMS ($n = 57$) (*D*).

in the number of SELs and T2 volume of SELs between RRMS and SPMS were not significant ($P = .17$ and $P = .23$, respectively). The proportion of baseline total nonenhancing T2 lesion burden identified as SELs was similar between patients with RRMS and SPMS (Fig 1*D*).

Baseline Level and Longitudinal Change in Tissue Integrity in SELs and Non-SELs of Patients with RRMS and SPMS, as Measured by nMTR and DTI-RD

SELs at baseline had a lower nMTR (expressed as an nMTR unit) versus non-SELs in patients with RRMS and SPMS (median, −0.67 versus −0.46, $P < .001$, and median, −1.01 versus −0.62, $P < .001$, respectively; Fig 2*A*) and a greater DTI-RD (median, 0.98 versus 0.88×10^{-3} mm^2/s, $P < .001$, and median, 1.07 versus 0.96×10^{-3} mm^2/s, $P < .001$, respectively; Fig 3*A*); means and medians were computed at the patient level. Baseline nMTR and DTI-RD parameters were reflective of more severe alterations of tissue integrity in patients with SPMS compared with RRMS, both in SELs and non-SELs (Fig 2*A* and 3*A*).

An assessment of change from baseline to week 72 showed that SELs were affected by significantly more tissue damage across time compared with non-SELs, as measured by an nMTR decrease and DTI-RD increase in both MS types—RRMS ($P < .001$ for both; Fig 2*B*) and SPMS ($P < .001$ and $P < .001$, respectively; Fig 3*B*). Most important, the differences in change in nMTR and DTI-RD from baseline were significant between SELs and non-SELs as of week 24 in the pooled RRMS-SPMS population ($P < .001$ for both). However, despite this difference in the severity of longitudinal tissue damage with time, at the individual patient level, we observed a mild-to-moderate positive correlation between SELs and non-SELs with regard to changes in nMTR (Spearman correlation = 0.39, $P < .001$, pooled RRMS-SPMS population) and DTI-RD (Spearman correlation = 0.56, $P < .001$, pooled RRMS-SPMS population) from baseline to week 72.

Although tissue-integrity alteration was significantly more pronounced in SELs from patients with SPMS than RRMS at baseline, the longitudinal tissue damage, as indicated by an nMTR decrease and DTI-RD increase with time (baseline to week 72) was similar in SELs from patients with RRMS and SPMS (Figs 2*C* and 3*C*).

A subtle and similar increase in DTI-RD from baseline to week 72 in patients with RRMS and SPMS was observed in non-SELs of chronic white matter lesions (Fig 3*C*). In contrast, there were directionally opposite trends in changes from baseline in

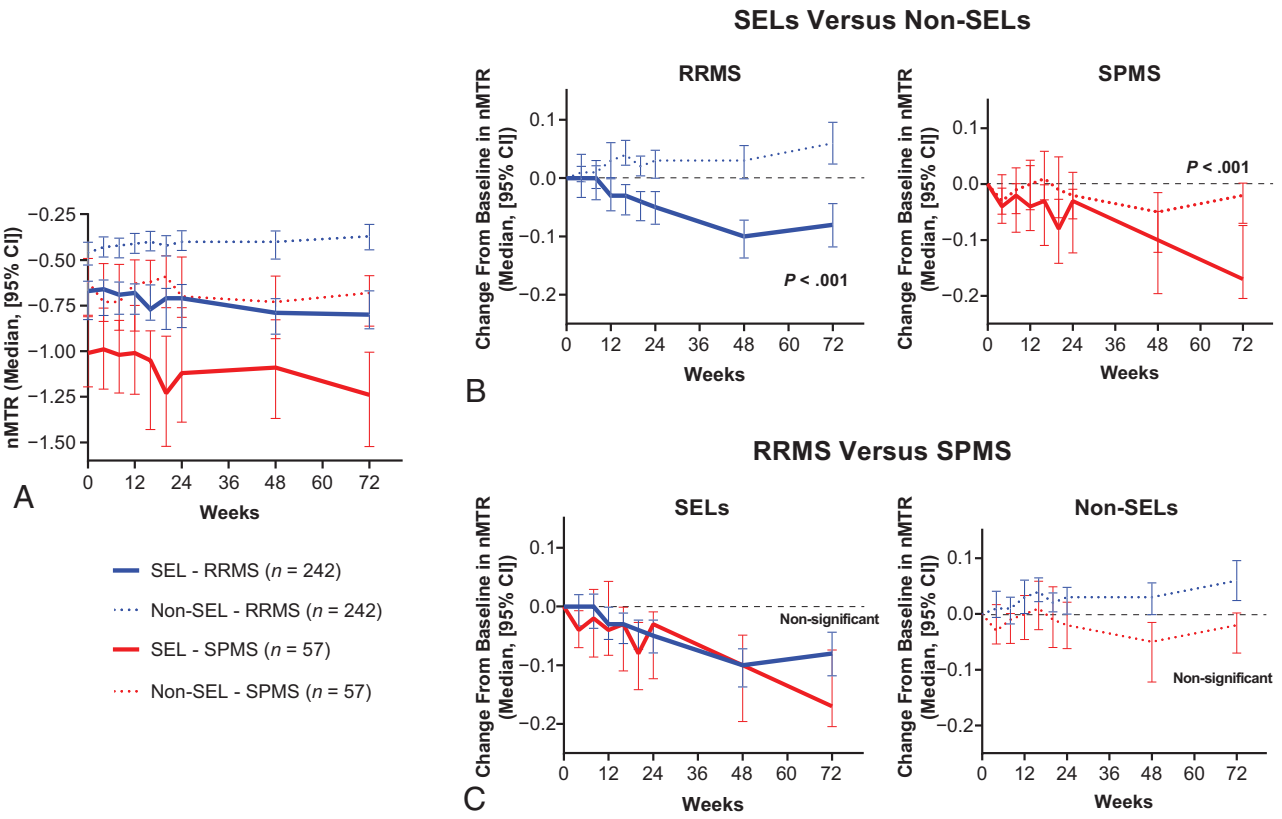

FIG 2. Change in nMTR in chronic white matter lesions. *A*, nMTR across time. *B*, Comparison of change from baseline in nMTR to week 72 between SELs and non-SELs in patients with RRMS and SPMS. *C*, Comparison of change from baseline in nMTR to week 72 between patients with RRMS and SPMS in SELs and non-SELs.

nMTR in non-SELs (albeit not statistically significant), with an increase in patients with RRMS and a decrease in patients with SPMS (Fig 2*C*). Overall, the findings from a comparison of baseline and longitudinal changes in nT1 intensity in SELs and non-SELs from patients with RRMS and SPMS were similar to aforementioned observations derived from the DTI-RD analysis (On-line Figure); these replicated previous findings that characterized T1-weighted normalized intensity changes in SELs versus non-SELs of chronic white matter lesions from patients with relapsing and primary-progressive forms of MS.[12]

An example of lesion-level chronic tissue damage, as measured by nT1 and nMTR intensity decrease and DTI-RD increase from baseline to week 72, is shown in Fig 4 and On-line Fig 2, where the longitudinal change with time can be visualized in a discrete SEL. Although a thorough analysis of spatial patterns of within-SEL intensity change was not conducted, examples of patterns consistent with ongoing demyelination at the lesion edge were observed.

DISCUSSION

This study further characterizes the nature of CNS tissue damage in chronic white matter MS lesions identified as SELs using serial conventional T1-weighted and T2-weighted MR imaging. Compared with non-SELs, SELs were previously shown to evolve independent of T1 gadolinium enhancement, demonstrate a lower T1 intensity at baseline, and exhibit a progressive decrease in T1 intensity with time, suggesting a progressive accumulation of neural tissue damage.[12]

We showed here that the longitudinal patterns of nMTR decrease and DTI-RD increase in SELs indicate a prominent contribution of chronic demyelination in those chronic active white matter MS lesions, though axonal loss may also be present. The overt consistency between longitudinal changes in nT1 intensity, nMTR, and DTI-RD in SELs and non-SELs with time provides evidence that nT1 intensity, though not a specific marker of myelin, could serve as a potential readout of chronic tissue damage in the absence of MTR and DTI acquisitions. Such nT1 intensity–based measures of CNS tissue integrity in SELs and non-SELs, separately, may provide value in clinical trials evaluating the effect of potential remyelination therapies.

The extent to which chronic demyelination in SELs evolves with an inside-out lesion-level pattern and its relationship to activated microglia/macrophage–mediated inflammatory processes on the lesion edge and/or to potential diffusible factors inherent to the scarce T- and B-cells (expected to populate the core of SELs within perivascular cuffs) need to be further investigated.[7] Quantitative susceptibility mapping imaging[27–31] should be used to assess the relation of SELs detected on MR imaging to the iron rim at the edge of chronic active lesions, as reported in pathologic studies, though only a subset of smoldering lesions appear to have iron/zinc rims.[14,15] The potential neuropathologic correlates of SELs warrant further investigation. However, the observed character of longitudinal nMTR, DTI-RD, and nT1 intensity features of change

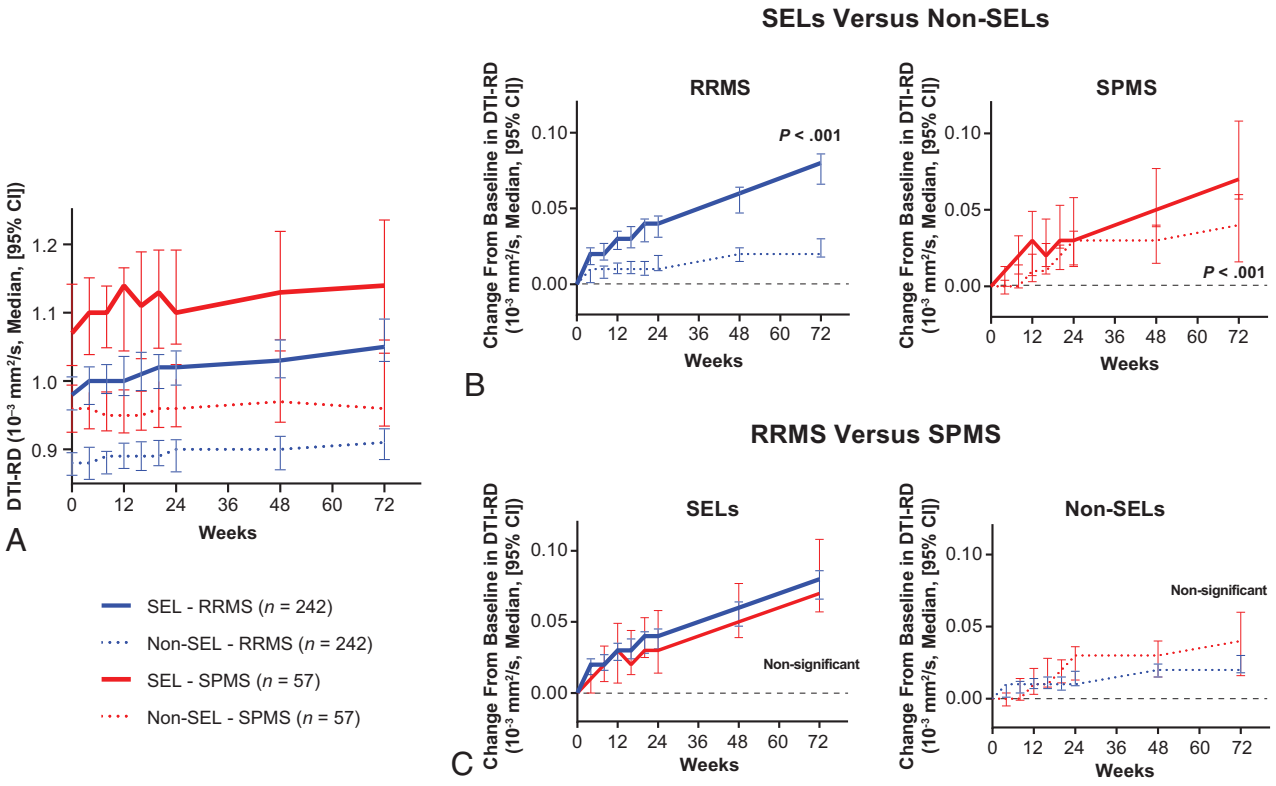

FIG 3. Change in DTI-RD in chronic white matter lesions. *A*, DTI-RD with time. *B*, Comparison of change from baseline in DTI-RD to week 72 between SELs and non-SELs in patients with RRMS and SPMS. *C*, Comparison of change from baseline in DTI-RD to week 72 between patients with RRMS and SPMS in SELs and non-SELs.

in tissue integrity in SELs may suggest that common mechanisms drive progressive demyelination in chronic white matter lesions across relapsing and progressive clinical presentations of the MS disease continuum. Furthermore, the correlation between the different rates of overall tissue demyelination observed in SELs and non-SELs, as measured by nMTR and DTI-RD, may indicate that a similar underlying pathology is diffusely at play throughout chronic white matter MS lesions, with maximal severity related to chronic lesion expansion in SELs.

The observed trend of nMTR increase in non-SELs of patients with RRMS suggests that remyelination may occur in chronic white matter lesions; however, a voxel-based approach would be needed to further address this hypothesis. Alternatively, the nMTR increase from baseline in non-SELs of patients with RRMS might be explained by the early resolution of inflammation and/or potential remyelination within foci of recent acute lesions, which might have formed before baseline but might still be a part of the baseline nonenhancing T2-hyperintense lesion tissue. In patients with radiologically isolated syndrome, acute and chronic demyelination may coexist from the onset of MS, irrespective of subsequent clinical phenotypes.[32] Although acute white matter MS lesions may be more amenable to remyelination owing to greater preservation of axons and lesser gliosis, spontaneous remyelination appears to be elusive in chronic active demyelinating lesions, which may represent a key driver of disability accumulation.[6,13,33] Further lesion-level spatiotemporal analyses of advanced and potentially multimodal brain MR imaging biomarkers of remyelination in SELs and non-SELs of chronic white matter lesions may help advance the understanding of putative associations between pathobiologic mechanisms of chronic demyelination, axonal loss, and remyelination failure.

The findings presented here have certain limitations. The current work did not investigate the potential impact of opicinumab versus placebo on chronic white matter lesion tissue integrity, which will be assessed more adequately in the Efficacy and Safety of BIIB033 (Opicinumab) as an Add-on Therapy to Disease-Modifying Therapies in Relapsing Multiple Sclerosis (AFFINITY) study (NCT03222973). Results should be interpreted with caution and may not fully reflect the natural history of changes in nMTR and DTI-RD in SELs and non-SELs of patients with RRMS and SPMS. The binary classification between SELs and non-SELs is somewhat artificial; longitudinal trajectories of tissue damage observed in non-SELs suggest that there may be a gradation of "activity" within chronic white matter MS lesions. Future work is needed to optimize SEL detection methods and further inform the understanding of spatiotemporal lesion-level patterns of tissue alteration in SELs by exploring alternative constancy/linearity and concentricity factor constraints of slow/chronic expansion detection criteria.

Furthermore, subsets of chronic active lesions that may shrink with time are not identified by the SEL detection method. The

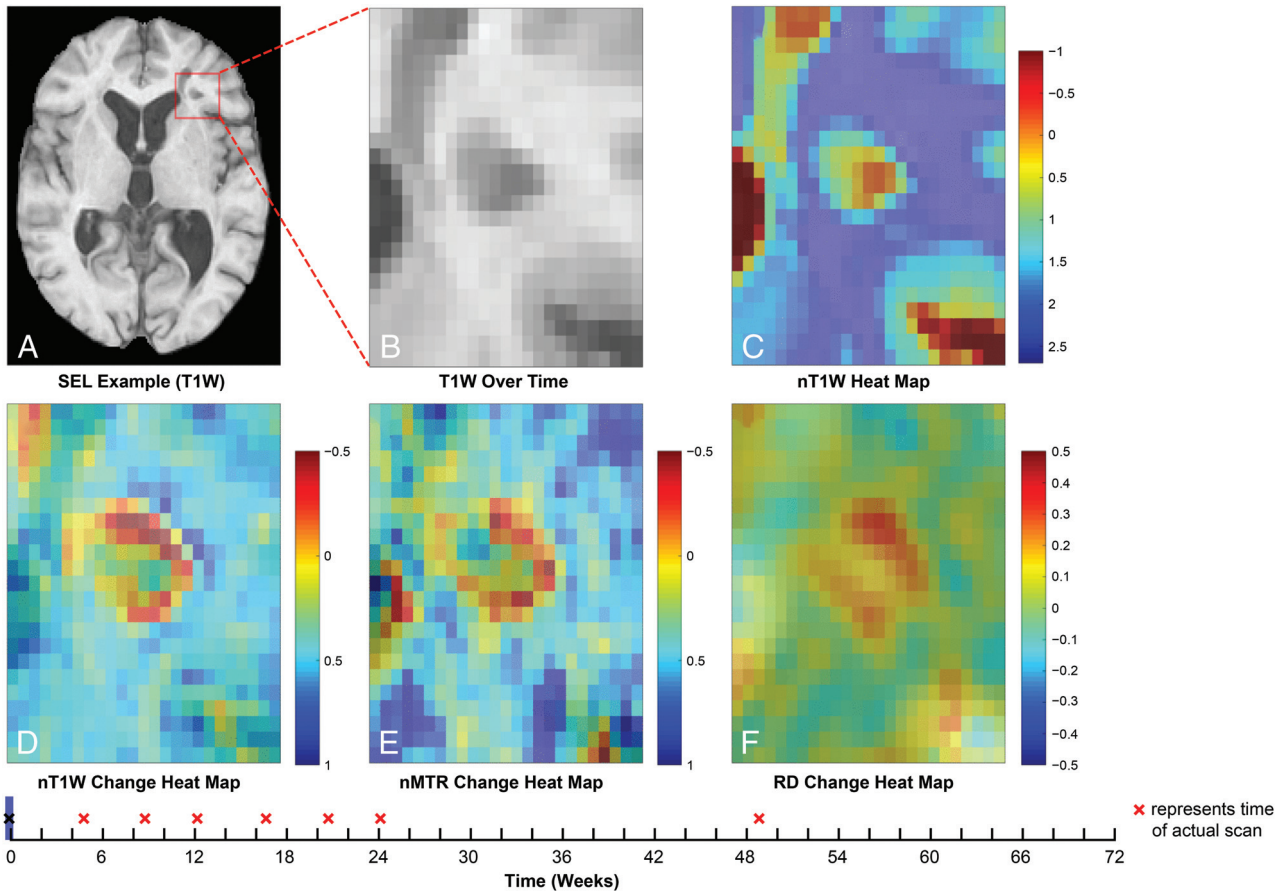

FIG 4. Example of lesion-level distribution of longitudinal tissue damage within SELs. Heat maps for normalized T1WI intensity and normalized T1WI (nT1WI), nMTR, and DTI-RD intensity change are based on linear modeling of intensity with time. Red "×" labels represent time of brain MR imaging scanning acquisitions. See On-line video for an animated version of this figure.

SEL quantification algorithm currently does not accommodate potential contraction at the lesion center across time, which is known to occur, especially in the longer term,[34] and underscores that the primary pathologic process in chronically evolving lesions (even those described by pathologists as "slowly expanding") is likely to include tissue loss. A recent study showed that chronic active lesions detected by the presence of a paramagnetic rim on high-field susceptibility-based MR imaging do not shrink slowly as other lesions do, but typically enlarge, similar to SELs, owing to ongoing demyelination (confirmed by pathologic assessment). Such chronic active/slowly expanding/smoldering MS lesions are associated with a more aggressive disease course[35] and disability progression[13] and should, therefore, be consistently assessed in MS clinical trials targeting chronic inflammation and remyelination.

CONCLUSIONS

Patterns of longitudinal change in nMTR and DTI-RD in SELs were consistent with progressive demyelination and tissue loss, as seen in smoldering white matter MS plaques. The consistency between longitudinal changes in nT1 intensity, nMTR, and DTI-RD in SELs and non-SELs with time suggests that nT1 intensity, though not a specific marker of myelin, could be a surrogate measure of chronic tissue damage in the absence of MTR and DTI acquisitions and may provide value in clinical trials evaluating the effect of potential remyelination and/or antiprogressive MS therapies.

ACKNOWLEDGMENTS

We thank all patients, their families, and the investigators who participated in SYNERGY. We also thank NeuroRx Research for evaluation of MR imaging scans. Editorial support for the preparation of this manuscript was provided by Excel Scientific Solutions.

Disclosures: Colm Elliott—*UNRELATED*: *Employment*: NeuroRx Research, *Comments*: full-time employee. Douglas L. Arnold—*UNRELATED*: *Personal Fees*: Acorda Therapeutics, Albert Charitable Trust, Biogen, Celgene, Roche, GeNeuro, Frequency Therapeutics, MedDay Pharma, Merck Serono, Novartis, Sanofi-Aventis, Wave Life Sciences; *Grant*: Biogen, Immunotec, Novartis; *Other*: NeuroRx Research, *Comments*: equity interest. Chunlei Ke—*UNRELATED*: *Employment*: Biogen; *Stock/Stock Options*: Biogen. Li Zhu—*UNRELATED*: *Employment*: Biogen; *Stock/Stock Options*: Biogen. Ih Chang—*UNRELATED*: former employee of and hold stock in Biogen. Ellen Cahir-McFarland—*UNRELATED*: *Other*: Biogen, *Comments*: employee who holds stock. Elizabeth Fisher—*UNRELATED*: *Employment*: Biogen, *Comments*: full-time employee; *Stock/Stock Options*: Biogen. Bing Zhu—*UNRELATED*: *Employment*: Biogen; *Stock/Stock Options*: Biogen. Sarah Gheuens—*UNRELATED*: former employee of and hold stock in Biogen; currently an employee of and hold stock in Agios Pharmaceuticals. Matthew Scaramozza—*UNRELATED*: *Employment*: Biogen, *Comments*: full-time salaried employee; *Stock/Stock Options*: Biogen, *Comments*: I received stock awards from Biogen as an employee and purchased stock under an employee stock purchase plan; *Travel/Accommodations/Meeting*

Expenses Unrelated to Activities Listed: Biogen, *Comments*: As an employee of Biogen, the company has paid for me to attend annual conferences in 2018 and 2019 (AAN and ECTRIMS). Nathalie Franchimont—*UNRELATED*: *Employment*: Biogen; *Stock/Stock Options*: Biogen, *Comments*: shareholder. Shibeshih Belachew—*UNRELATED*: *Employment*: Biogen; *Stock/Stock Options*: Biogen, *Comments*: shareholder. *Money paid to the institution.

REFERENCES

1. Frischer JM, Weigand SD, Guo Y, et al. **Clinical and pathological insights into the dynamic nature of the white matter multiple sclerosis plaque.** *Ann Neurol* 2015;78:710–21 CrossRef Medline
2. Chawla S, Kister I, Wuerfel J, et al. **Iron and non-iron-related characteristics of multiple sclerosis and neuromyelitis optica lesions at 7T MRI.** *AJNR Am J Neuroradiol* 2016;37:1223–30 CrossRef Medline
3. Kilsdonk ID, Wattjes MP, Lopez-Soriano A, et al. **Improved differentiation between MS and vascular brain lesions using FLAIR* at 7 Tesla.** *Eur Radiol* 2014;24:841–49 CrossRef Medline
4. Dal-Bianco A, Grabner G, Kronnerwetter C, et al. **Slow expansion of multiple sclerosis iron rim lesions: pathology and 7 T magnetic resonance imaging.** *Acta Neuropathol* 2017;133:25–42 CrossRef Medline
5. Kuhlmann T, Ludwin S, Prat A, et al. **An updated histological classification system for multiple sclerosis lesions.** *Acta Neuropathol* 2017;133:13–24 CrossRef Medline
6. Luchetti S, Fransen NL, van Eden CG, et al. **Progressive multiple sclerosis patients show substantial lesion activity that correlates with clinical disease severity and sex: a retrospective autopsy cohort analysis.** *Acta Neuropathol* 2018;135:511–28 CrossRef Medline
7. Machado-Santos J, Saji E, Tröscher AR, et al. **The compartmentalized inflammatory response in the multiple sclerosis brain is composed of tissue-resident CD8+ T lymphocytes and B cells**. *Brain* 2018;141:2066–82 CrossRef Medline
8. Filippi M, Rocca MA, Barkhof F, et al; Attendees of the Correlation between Pathological MRI Findings in MS Workshop. **Association between pathological and MRI findings in multiple sclerosis.** *Lancet Neurol* 2012;11:349–60 CrossRef Medline
9. Absinta M, Sati P, Reich DS. **Advanced MRI and staging of multiple sclerosis lesions.** *Nat Rev Neurol* 2016;12:358–68 CrossRef Medline
10. Absinta M, Sati P, Schindler M, et al. **Persistent 7-Tesla phase rim predicts poor outcome in new multiple sclerosis patient lesions.** *J Clin Invest* 2016;126:2597–609 CrossRef Medline
11. Filippi M, Preziosa P, Banwell BL, et al. **Assessment of lesions on magnetic resonance imaging in multiple sclerosis: practical guidelines.** *Brain* 2019;142:1858–75 CrossRef Medline
12. Elliott C, Wolinsky JS, Hauser SL, et al. **Slowly expanding/evolving lesions as a magnetic resonance imaging marker of chronic active multiple sclerosis lesions.** *Mult Scler* 2019;25:1915–25 CrossRef Medline
13. Elliott C, Belachew S, Wolinsky JS, et al. **Chronic white matter lesion activity predicts clinical progression in primary progressive multiple sclerosis.** *Brain* 2019;142:2787–99 CrossRef Medline
14. Haacke EM, Makki M, Ge Y, et al. **Characterizing iron deposition in multiple sclerosis lesions using susceptibility weighted imaging.** *J Magn Reson Imaging* 2009;29:537–44 CrossRef Medline
15. Popescu BF, Frischer JM, Webb SM, et al. **Pathogenic implications of distinct patterns of iron and zinc in chronic MS lesions.** *Acta Neuropathol* 2017;134:45–64 CrossRef Medline
16. Barkhof F, Brück W, De Groot CJ, et al. **Remyelinated lesions in multiple sclerosis: magnetic resonance image appearance.** *Arch Neurol* 2003;60:1073–81 CrossRef Medline
17. Schmierer K, Scaravilli F, Altmann DR, et al. **Magnetization transfer ratio and myelin in postmortem multiple sclerosis brain.** *Ann Neurol* 2004;56:407–15 CrossRef Medline
18. Merkler D, Boretius S, Stadelmann C, et al. **Multicontrast MRI of remyelination in the central nervous system.** *NMR Biomed* 2005;18:395–403 CrossRef Medline
19. Chen JT, Collins DL, Atkins HL, et al; Canadian MS/BMT Study Group. **Magnetization transfer ratio evolution with demyelination and remyelination in multiple sclerosis lesions.** *Ann Neurol* 2008;63:254–62 CrossRef Medline
20. Fox RJ, Cronin T, Lin J, et al. **Measuring myelin repair and axonal loss with diffusion tensor imaging.** *AJNR Am J Neuroradiol* 2011;32:85–91 CrossRef Medline
21. Klawiter EC, Schmidt RE, Trinkaus K, et al. **Radial diffusivity predicts demyelination in ex vivo multiple sclerosis spinal cords.** *Neuroimage* 2011;55:1454–60 CrossRef Medline
22. Cadavid D, Mellion M, Hupperts R, et al; SYNERGY Study Investigators**. Safety and efficacy of opicinumab in patients with relapsing multiple sclerosis (SYNERGY): a randomised, placebo-controlled, phase 2 trial.** *Lancet Neurol* 2019;18:845–56 CrossRef Medline
23. Francis SJ. ***Automatic Lesion Identification in MRI of Multiple Sclerosis Patients.*** Thesis. Division of Neuroscience, McGill University. 2004
24. Nakamura K, Guizard N, Fonov VS, et al. **Jacobian integration method increases the statistical power to measure gray matter atrophy in multiple sclerosis.** *Neuroimage Clin* 2014;4:10–17 CrossRef Medline
25. Avants BB, Epstein CL, Grossman M, et al. **Symmetric diffeomorphic image registration with cross-correlation: evaluating automated labeling of elderly and neurodegenerative brain.** *Med Image Anal* 2008;12:26–41 CrossRef Medline
26. Rousseeuw P, Van Driessen K. **Computing LTS regression for large data sets.** *Data Mining and Knowledge Discovery* 2006;12:29–45 CrossRef
27. Chen W, Gauthier SA, Gupta A, et al. **Quantitative susceptibility mapping of multiple sclerosis lesions at various ages.** *Radiology* 2014;271:183–92 CrossRef Medline
28. Wisnieff C, Ramanan S, Olesik J, et al. **Quantitative susceptibility mapping (QSM) of white matter multiple sclerosis lesions: interpreting positive susceptibility and the presence of iron.** *Magn Reson Med* 2015;74:564–70 CrossRef Medline
29. Deh K, Ponath GD, Molvi Z, et al. **Magnetic susceptibility increases as diamagnetic molecules breakdown: myelin digestion during multiple sclerosis lesion formation contributes to increase on QSM.** *J Magn Reson Imaging* 2018;48:1281–87 CrossRef Medline
30. Yao Y, Nguyen TD, Pandya S, et al. **Combining quantitative susceptibility mapping with automatic zero reference (QSM0) and myelin water fraction imaging to quantify iron-related myelin damage in chronic active MS lesions.** *AJNR Am J Neuroradiol* 2018;39:303–10 CrossRef Medline
31. Zhang S, Liu Z, Nguyen TD, et al. **Clinical feasibility of brain quantitative susceptibility mapping.** *Magn Reson Imaging* 2019;60:44–51 CrossRef Medline
32. Suthiphosuwan S, Sati P, Absinta M, et al. **Paramagnetic rim sign in radiologically isolated syndrome.** *JAMA Neurol* 2020;77:653 CrossRef Medline
33. Kaunzner UW, Kang Y, Zhang S, et al. **Quantitative susceptibility mapping identifies inflammation in a subset of chronic multiple sclerosis lesions.** *Brain* 2019;142:133–45 CrossRef Medline
34. Sethi V, Nair G, Absinta M, et al. **Slowly eroding lesions in multiple sclerosis.** *Mult Scler* 2017;23:464–72 CrossRef Medline
35. Absinta M, Sati P, Masuzzo F, et al. **Association of chronic active multiple sclerosis lesions with disability in vivo.** *JAMA Neurol* 2019;76:1474–83 CrossRef Medline